

## Time-Varying Jamming Modeling and Classification

Lei Zhang, Jian Ren, and Tongtong Li

**Abstract**—In this correspondence, we provide a general jamming model, through which all the existing models can be summarized and extended to the time-varying case under one unified framework. We analyze the time varying jamming power spectral density, and propose a new jamming classification scheme by introducing the concepts of time-varying jamming coherence time and time-frequency jamming coherence bandwidth. Specific methods on power spectrum estimation are provided for time-varying jamming that is stationary or locally stationary.

**Index Terms**—Cognitive jamming, power spectrum, time-frequency analysis.

### I. INTRODUCTION

One of the most commonly used techniques for limiting the effectiveness of an opponent's communications is referred to as *jamming*. Intentional jamming, also known as hostile jamming, intends to disable the legitimate transmission by saturating the receiver with noise or false information through deliberate radiation of radio signals, and thus significantly decreasing the signal-to-interference-plus-noise ratio (SINR). In literature, jamming signals are generally categorized into the following three classes.

- i) *Band jamming*, generally modeled as a zero-mean wide sense stationary Gaussian random process with a flat power spectral density (PSD) over the bandwidth of interest. Band jamming is further classified into *full-band jamming* [1] and *partial-band jamming* [2].
- ii) *Tone jamming*, typically a sinusoid waveform whose power is concentrated on the carrier frequency. Tone jamming includes single-tone jamming and multi-tone jamming [3].
- iii) *Partial-time jamming*, modeled as a two-state Markov process, for which the jammer is on in state 1, and is off in state 0. State 1 occurs with probability of  $\rho$ , and state 0 occurs with probability  $(1 - \rho)$  [4].

Existing work on jamming detection and jamming prevention was generally targeted at a particular jamming model at a time. That is, the jamming pattern is assumed to be known and invariant during the signal transmission period, see [5], [6], for example. In practice, however, the jammer may very likely switch frequently from one pattern to another, with each jamming pattern only lasting a very short period of time. In other words, the jammer may launch smart, cognitive jamming, also known as adaptive jamming or time-varying jamming. Note that no particular anti-jamming system is effective under all jamming attacks. For optimum jamming mitigation, the transmitter has to be cognitive as well. Cognitive jamming modeling and classification are critical for dynamic anti-jamming system design.

Manuscript received October 06, 2011; revised January 20, 2012; accepted March 20, 2012. Date of publication April 05, 2012; date of current version June 12, 2012. The associate editor coordinating the review of this manuscript and approving it for publication was Dr. Maja Bystrom. This research is partially supported by NSF under awards CNS-0746811 and CNS-1117831.

L. Zhang is with Marvell Semiconductor, Inc., Santa Clara, CA 95054 USA (e-mail: lei@marvell.com).

J. Ren and T. Li are with the Department of Electrical and Computer Engineering, Michigan State University, East Lansing, MI 48824 USA (e-mail: renjian@msu.edu; tongli@msu.edu).

Color versions of one or more of the figures in this correspondence are available online at <http://ieeexplore.ieee.org>.

Digital Object Identifier 10.1109/TSP.2012.2193574

This correspondence focuses on cognitive jamming modeling and classification based on time-frequency analysis. We introduce the concepts of time-varying jamming coherence time and time-frequency jamming coherence bandwidth. By comparing the time-varying jamming coherence time with the signal symbol period, we classify the jamming into fast jamming and slow jamming; By comparing the time-frequency jamming coherence bandwidth with the signal bandwidth, we classify the jamming into flat jamming and frequency selective jamming. Note that at one time instant, the jamming coherence bandwidth may vary from one frequency to another. Therefore, a multi-band signal may experience flat jamming and frequency selective jamming simultaneously at different frequency bands. Algorithms based on time-frequency analysis and approximation theory are developed to estimate the time-varying jamming coherence time and the time-frequency coherence bandwidth for both stationary and locally stationary jamming. Simulation results are provided to demonstrate the proposed approaches.

### II. COGNITIVE JAMMING MODELING AND CLASSIFICATION

In this section, we will focus on the characterization of hostile jamming through time-frequency analysis of the jamming statistics.

#### A. Jamming Modeling Using Time-Varying Power Spectral Density

We start with a single-input single-output AWGN channel. Let  $s(t)$  be the transmitted signal, then the received signal can be written as

$$r(t) = s(t) + n(t) + J(t) \quad (1)$$

where  $n(t)$  is the white Gaussian noise,  $J(t)$  represents the hostile jamming signal.  $J(t)$  can either be stationary or nonstationary. Let  $R_J(t, \tau) = E\{J(t + \tau)J(t)\}$  be the autocorrelation function of  $J(t)$ . The time-varying power spectral density is defined as

$$S_J(t, f) = \mathcal{F}\{R_J(t, \tau)\} = \int_{-\infty}^{\infty} R_J(t, \tau) e^{-j2\pi f\tau} d\tau, \quad (2)$$

The time-varying jamming power is given by  $P_J(t) = \int_{-\infty}^{\infty} S_J(t, f) df$ . We assume that  $P_J(t)$  is finite and  $P_J(t) \leq P_{J,\max}$ , where  $P_{J,\max}$  is the maximum jamming power. The reason that we allow the jamming power to be time-varying, rather than always using the total available jamming power, is because that strong jamming that uses the whole jamming power may not always be the worst jamming [7]. If  $J(t)$  is wide-sense stationary, then  $R_J(t, \tau)$ ,  $S_J(t, f)$  and  $P_J(t)$  all become time-invariant.

It turns out that *all the existing jamming models can be characterized using the time-varying power spectral density*,  $S_J(t, f)$ . In fact, let  $f_0$  and  $f_1$  be the start and ending frequency of the available frequency band, respectively,  $[t_0, t_1]$  the time duration period of the message signal, and  $P_J$  the constant jamming power.

- If  $S_J(t, f) = \frac{P_J}{f_1 - f_0} \triangleq N_J, \forall f \in [f_0, f_1], \forall t \in [t_0, t_1]$ , then  $J(t)$  with PSD  $S_J(t, f)$  is reduced to the traditional full-band jamming. Partial-band jamming can be defined in a similar manner.
- If  $S_J(t, f) = P_J \delta(f - f_k), \forall t \in [t_0, t_1]$ , where  $f_k \in [f_0, f_1]$  and  $\delta$  is the Dirac delta function, then we obtain the single-tone jamming. For multi-tone jamming,

$$S_J(t, f) = \sum_{k=1}^K P_J(t, k) \delta(f - f_k), \text{ s.t. } \sum_{k=1}^K P_J(t, k) = P_J \quad (3)$$

where  $K$  is the number of jamming tones, and  $P_J(t, k)$  stands for the jamming power allocated for the  $k$ th tone  $f_k$ .

- If  $\forall f \in [f_0, f_1]$ ,

$$S_J(t, f) = \begin{cases} 0, & \text{if } t \in [t_0, t_m) \text{ or } t \in (t_n, t_1] \\ \frac{P_J}{f_1 - f_0}, & \text{if } t \in [t_m, t_n] \end{cases} \quad (4)$$

where  $t_m$  and  $t_n$  ( $t_m \leq t_n$ ) are certain intermediate time instants within  $[t_0, t_1]$ , then we obtain the partial-time jamming.

Motivated by the observations above, we propose to model  $J(t)$  through 2D analysis of  $R_J(t, \tau)$  and its Fourier transform  $S_J(t, f)$ .

### B. Jamming Classification Based on Time-frequency Analysis

In this section, we introduce the concepts of *time-varying jamming coherence time* and *time-frequency jamming coherence bandwidth* for  $J(t)$ .

- *Time-varying jamming coherence time*: For a given time instant  $t$ , let  $[0, T_c(t)]$  be the period over which  $R_J(t, \tau)$  is essentially non-zero and flat. This implies that  $J(t + \tau)$  and  $J(t)$  are highly correlated when  $\tau \leq T_c(t)$ . We define  $T_c(t)$  as the *time-varying jamming coherence time* of  $J(t)$ .  $T_c(t)$  is used to characterize the time-varying nature of  $J(t)$  in the time domain. In other words,  $T_c(t)$  is a statistical measure of the time duration over which  $J(t)$  is essentially invariant.
- *Time-frequency jamming coherence bandwidth*: For a given time instant  $t$  and frequency  $v$ , let  $[v - \frac{B_c(t, v)}{2}, v + \frac{B_c(t, v)}{2}]$  be the frequency range over which the magnitude of the time-varying jamming PSD,  $|S_J(t, f)|$ , is essentially nonzero and can be considered to be flat. That is, at time instant  $t$ , two frequency components around  $v$  with separation greater than  $B_c(t, v)$  are affected differently by the jamming. We define  $B_c(t, v)$  as the *time-frequency jamming coherence bandwidth at time  $t$  and frequency  $v$* .

Let  $T_s$  and  $B_s$  be the symbol period and bandwidth of the information signal, respectively, where  $T_s$  and  $B_s$  can be time-varying as well, such as in adaptive transmitters. We further introduce the following jamming classification criteria.

- For any given time instant  $t$ , if  $T_s > T_c(t)$ , then it means that the jamming changes rapidly within the symbol duration of the signal, we say that the signal is experiencing *fast jamming at time  $t$* . Otherwise, we say that the signal is experiencing *slow jamming*.
- For any given time instant  $t$ , let  $f_c(t)$  be the center frequency of the signal. If  $B_c(t, f_c(t)) > B_s$ , that is, the jamming coherence bandwidth at  $v = f_c(t)$  is larger than the signal bandwidth, we say that the signal is experiencing *flat jamming at time  $t$* . Otherwise, we say that the signal is experiencing *frequency selective jamming*. For multi-carrier signals,  $B_c(t, v)$  needs to be evaluated at each carrier frequency. Therefore, a multi-band signal may experience flat jamming and frequency selective jamming simultaneously at different frequency bands.

### III. ESTIMATION OF TIME-VARYING JAMMING COHERENCE TIME AND TIME-FREQUENCY JAMMING COHERENCE BANDWIDTH

For jamming classification, we consider two scenarios: i)  $J(t)$  is stationary and ii)  $J(t)$  is locally stationary [8], [9], which means that for any  $t$ , there exists a time interval of size  $l(t)$ ,  $[t - \frac{l(t)}{2}, t + \frac{l(t)}{2}]$ , such that  $J(t)$  can be approximated by a stationary process within this interval. The size of the intervals,  $l(t)$  may change with time  $t$ . This assumption is reasonable in the sense that a particular jamming pattern may last for a short time and then the jammer switches to another pattern.

#### A. Stationary Jamming

When  $J(t)$  is stationary, the autocorrelation function  $R_J(t, \tau) = E\{J(t + \tau)J(t)\}$  and its Fourier transform  $S_J(t, f)$  are both independent of  $t$ . We have  $R_J(\tau) = E\{J(t + \tau)J(t)\}$  and  $S_J(f) =$

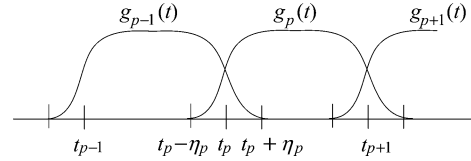


Fig. 1. An example of window functions.

$\mathcal{F}\{R_J(\tau)\} = \int_{-\infty}^{\infty} R_J(\tau)e^{-j2\pi f\tau} d\tau$ . In this case,  $T_c(t)$  and  $B_c(t, v)$  become time-invariant, and are denoted as  $T_c$  and  $B_c(v)$ , respectively.

By definition,  $[0, T_c]$  is the period over which  $R_J(\tau)$  is flat and essentially nonzero. That is,

$$|R_J(\tau)| > \alpha_0 R_J(0) \quad (5)$$

where  $\alpha_0 \in [0.5, 0.95]$  is a predefined constant for coherence time estimation.

For any given frequency  $v$ , let  $[v - \frac{B_c(v)}{2}, v + \frac{B_c(v)}{2}]$  be the frequency range over which  $S_J(f)$  is essentially nonzero and can be considered to be flat. Consider the case that  $S_J(f)$  has only one main lobe in the positive frequency range, centered at  $f_c$ . i) When  $f_c = 0$ ,  $J(t)$  is a baseband stationary process. For  $v = 0$ ,  $B_c(0)$  can be estimated through

$$\int_{-\frac{B_c(0)}{2}}^{\frac{B_c(0)}{2}} |S_J(f)|^2 df \geq \alpha_1 \|S_J\|_2^2 \quad (6)$$

where  $\alpha_1 \in [0.5, 0.95]$  is a predefined constant for coherence bandwidth estimation [10]. For any  $v \neq 0$ ,  $B_c(v)$  can be estimated from  $B_c(0)$  as  $B_c(v) = B_c(0) - 2|v|$ , if  $0 < |v| < \frac{B_c(0)}{2}$ ;  $B_c(v) = 0$ , if  $|v| \geq \frac{B_c(0)}{2}$ . ii) When  $f_c > 0$ ,  $J(t)$  is a passband stationary process. For  $|v| = f_c$ ,  $B_c(v)$  can be estimated through

$$\int_{f_c - \frac{B_c(v)}{2}}^{f_c + \frac{B_c(v)}{2}} |S_J(f)|^2 df \geq \frac{\alpha_1}{2} \|S_J\|_2^2. \quad (7)$$

For  $|v| \neq f_c$ ,  $B_c(v)$  can be estimated from  $B_c(f_c)$  as:  $B_c(v) = B_c(f_c) - 2||v| - f_c|$ , if  $0 < ||v| - f_c| < \frac{B_c(f_c)}{2}$ ;  $B_c(v) = 0$ , if  $||v| - f_c| \geq \frac{B_c(f_c)}{2}$ .

#### B. Locally Stationary Jamming

1) *Definition*: First, partition the active time axis into intervals  $[t_p, t_{p+1}]$  of size  $l_p = t_{p+1} - t_p$ , with  $\lim_{p \rightarrow -\infty} t_p = -\infty$  and  $\lim_{p \rightarrow \infty} t_p = \infty$ . We cover each interval  $[t_p, t_{p+1}]$  with a window function  $g_p(t)$ . As shown in Fig. 1, we construct the window function  $g_p(t)$  such that it satisfies the following conditions: i) For  $\forall p \in \mathbb{Z}$ , the support of  $g_p(t)$  only intersects with the support of  $g_{p-1}(t)$  and  $g_{p+1}(t)$ . The supports of  $g_p(t)$  and  $g_{p-1}(t)$  intersects in  $[t_p - \eta_p, t_p + \eta_p]$ . ii)  $g_p(t)$  and  $g_{p-1}(t)$  are symmetric with respect to  $t_p$ , i.e.,  $g_p(t) = g_{p-1}(2t_p - t)$  over  $[t_p - \eta_p, t_p + \eta_p]$ . iii) For  $\forall t \in \mathbb{R}$ ,  $\sum_{p=-\infty}^{\infty} |g_p(t)|^2 = 1$ . It can be shown that under these three conditions, the local cosine family defined by

$$\left\{ \phi_{p,k}(t) = g_p(t) \sqrt{\frac{2}{l_p}} \cos \left[ \frac{\pi(k+1/2)}{l_p} (t - t_p) \right] \right\}_{k \in \mathbb{N}, p \in \mathbb{Z}} \quad (8)$$

formulates an orthonormal basis of  $L^2(\mathbb{R})$  [11]. From (8), we can see that the support of  $\phi_{p,k}(t)$  is  $[t_p - \eta_p, t_{p+1} + \eta_{p+1}]$ , and its center frequency is  $\xi_{p,k} = \frac{\pi(k+1/2)}{l_p}$ .

For  $R_J(t, \tau) = E\{J(t + \tau)J(t)\}$ , let  $s = t + \tau$ , then  $R_J(t, \tau)$  can be rewritten as  $R_J(t, s) = E\{J(t)J(s)\}$ . For  $\forall f \in L^2(\mathbb{R})$ , define the covariance operator by

$$Tf(t) = \int_{-\infty}^{\infty} R_J(t, s)f(s)ds. \quad (9)$$

Following [11], locally stationary jamming processes can be defined as follows.

*Definition 1:* A jamming  $J(t)$  is said to be locally stationary if there exists a local cosine basis  $\{\phi_{p,k}(t)\}_{k \in \mathbb{N}, p \in \mathbb{Z}}$  such that for some constant  $\mu < 1$  and  $A > 0$ , we have that for all  $p \neq q$ ,

$$\frac{\max(l_p, l_q)}{\min(l_p, l_q)} \leq A|p - q|^\mu, \quad (10)$$

and for all  $n > 1$ , we can find a constant  $Q_n$  such that for all  $(p, q, j, k) \in \mathbb{Z}^2 \times \mathbb{N}^2$ ,

$$|\langle T\phi_{p,k}, \phi_{q,j} \rangle| \leq \frac{Q_n}{(1+|p-q|^n)(1+|\max(l_p, l_q)(\xi_{p,k} - \xi_{q,j})|^n)}.$$

Here,  $\{l_p\}$  specify the supports of  $\{\phi_{p,k}(t)\}$  and indicate the intervals over which  $J(t)$  is approximately stationary. Condition (11) implies that  $|\langle T\phi_{p,k}, \phi_{q,j} \rangle|$  decays rapidly as we increase  $|p - q|$  and  $|\xi_{p,k} - \xi_{q,j}|$ . This means that the operator  $T$  is “almost” diagonalized by  $\{\phi_{p,k}(t)\}$ . In other words, each  $\phi_{p,k}(t)$  is “almost” an eigenvector of  $T$ .

2) *Best Basis Search and Spectrum Estimation:* Let  $\{\phi_n(t)\}_{n \in \mathbb{N}}$  be an orthonormal basis of  $L^2(\mathbb{R})$ , which implies that for any  $f(t) \in L^2(\mathbb{R})$ ,  $f(t)$  can be decomposed as  $f(t) = \sum_{n \in \mathbb{N}} \langle f, \phi_n \rangle \phi_n(t)$ . It follows that  $Tf(t) = \sum_{n \in \mathbb{N}} \langle f, \phi_n \rangle T\phi_n(t)$ . That is, the operator  $T$  is completely determined by  $T\phi_n(t)$ . For any  $m \in \mathbb{N}$ ,

$$T\phi_m(t) = \sum_{n \in \mathbb{N}} \langle T\phi_m, \phi_n \rangle \phi_n(t). \quad (11)$$

Note that, in practice,  $Tf(t)$  can only be approximated by a finite sum. A natural question is: for a fixed number of items in the sum, which basis will result in the best approximation? Let  $\mathcal{D} = \{B^\gamma\}_{\gamma \in \Gamma}$  be a dictionary of orthonormal basis  $B^\gamma = \{\phi_n^\gamma\}_{n \in \mathbb{N}}$  of  $L^2(\mathbb{R})$ , indexed by  $\gamma \in \Gamma$  where  $\Gamma$  denotes the collection of all the index sets in the dictionary. Define  $B_K^\gamma$  as

$$\langle B_K^\gamma \phi_m^\gamma, \phi_n^\gamma \rangle = \begin{cases} \langle T\phi_m^\gamma, \phi_n^\gamma \rangle, & \text{if } |n - m| \leq K \\ 0, & \text{Otherwise.} \end{cases} \quad (12)$$

For a fixed  $K$ , the best basis is the one which minimizes the norm  $\|T - B_K^\gamma\|_s$ , defined as

$$\|T - B_K^\gamma\|_s = \sup_{\|f\|_2=1} \|(T - B_K^\gamma)f\|_2. \quad (13)$$

Since local cosine functions are approximate eigenvectors of the corresponding covariance operator  $T$ , we search the best basis in a dictionary of local cosine bases, with  $K = 0$  in (12) such that the operator  $T$  is diagonalized. Once the best basis  $\{\phi_n^{\gamma_0}\}_{n=1}^N$  is selected, we have

$$R_J(t, s) \approx \sum_{m=1}^N \sum_{n=1}^N E \{ \langle J, \phi_m^{\gamma_0} \rangle \langle J, \phi_n^{\gamma_0} \rangle \} \phi_m^{\gamma_0}(t) \phi_n^{\gamma_0}(s). \quad (14)$$

Following from (11) and (14), we have

$$R_J(t, s) \approx \sum_{m=1}^N \sum_{n=1}^N \langle T\phi_n^{\gamma_0}, \phi_m^{\gamma_0} \rangle \phi_m^{\gamma_0}(t) \phi_n^{\gamma_0}(s) \quad (15)$$

$$= \sum_{n=1}^N \langle T\phi_n^{\gamma_0}, \phi_n^{\gamma_0} \rangle \phi_n^{\gamma_0}(t) \phi_n^{\gamma_0}(s). \quad (16)$$

Let  $d_n = \langle T\phi_n^{\gamma_0}, \phi_n^{\gamma_0} \rangle = E \{ |\langle J, \phi_n^{\gamma_0} \rangle|^2 \}$ , then the time-varying auto-correlation function can be estimated as

$$R_J(t, \tau) \approx \sum_{n=1}^N d_n \phi_n^{\gamma_0}(t) \phi_n^{\gamma_0}(t + \tau). \quad (17)$$

Let  $x_n$  and  $\xi_n$  denote the center time and the center frequency corresponding to the local cosine function<sup>1</sup>  $\phi_n^{\gamma_0}$ , respectively. That is,

$$\phi_n^{\gamma_0}(t) = g_{x_n}(t) \cos(\xi_n t + \theta_n). \quad (18)$$

In the time domain, the smooth function  $g_{x_n}(t)$  is approximately nonzero and flat over the time support  $[x_n - \frac{l(x_n)}{2}, x_n + \frac{l(x_n)}{2}]$ . Assuming  $J(t)$  has a finite duration, and can be covered by  $P$  window functions  $\{g_p(t)\}_{p=1}^P$  associated with the best basis functions  $\{\phi_n^{\gamma_0}\}_{n=1}^N$ . Let  $\mathcal{N}_p$  denote the set of indexes for the best basis functions corresponding to  $g_p(t)$ . Then,  $g_{x_n}(t) = \sqrt{\frac{2}{l_p}} g_p(t)$  for any  $n \in \mathcal{N}_p$ , and  $\cup_{p=1}^P \mathcal{N}_p = \{1, \dots, N\}$ . We have

$$\hat{R}_J(t, \tau) = \sum_{p=1}^P \frac{2}{l_p} g_p(t) g_p(t + \tau) \times \left[ \sum_{n \in \mathcal{N}_p} \hat{d}_n \cos(\xi_n t + \theta_n) \cos(\xi_n t + \xi_n \tau + \theta_n) \right], \quad (19)$$

where  $\hat{d}_n = \frac{1}{Q} \sum_{q=1}^Q |\langle J^q, \phi_n^{\gamma_0} \rangle|^2$ . For any  $t$ ,  $T_c(t)$  can then be estimated from  $\hat{R}_J(t, \tau)$  using the method described in (5).

Taking Fourier transform on both sides of (19), we have

$$\hat{S}_J(t, f) = \sum_{p=1}^P \frac{1}{l_p} g_p(t) e^{j2\pi f t} \sum_{n \in \mathcal{N}_p} \hat{d}_n \cos(\xi_n t + \theta_n) \times \left[ G_p \left( f - \frac{\xi_n}{2\pi} \right) e^{j\theta_n} + G_p \left( f + \frac{\xi_n}{2\pi} \right) e^{-j\theta_n} \right] \quad (20)$$

where  $G_p(f) = \int_{-\infty}^{\infty} g_p(\tau) e^{-j2\pi f \tau} d\tau$ . For any  $t$  and  $v$ ,  $B_c(t, v)$  can be estimated from  $|\hat{S}_J(t, f)|$  using the method described in (6), (7).

### C. Binary Tree Based Basis Search Algorithm

We now discuss a practical binary tree based algorithm for fast “best basis” search.

1) *Dictionary Construction:* To reduce the complexity of the best basis search, a dictionary with admissible binary tree structure is preferred [12]. The admissible binary tree is defined by any binary tree whose nodes have either 0 or 2 branches. Each tree node corresponds to a time interval. Assume the jamming  $J(t)$  is observed over  $0 \leq t \leq M$ . The root of the tree corresponds to the whole time interval  $[0, M]$ . The left and right branch nodes correspond to the time interval  $[0, \frac{M}{2}]$  and  $[\frac{M}{2}, M]$ , respectively. Each node is further split until the tree depth  $N_D$  is reached. The node  $(p, j)$  at depth  $j$  and position  $p$  corresponds to the time interval  $[pM2^{-j}, (p+1)M2^{-j}]$ . The window function  $g_p^j(t)$  is used to cover the time interval corresponding to each node  $(p, j)$ . Given a smooth function  $\beta(t)$  which satisfies:  $\beta(t) = 0$  if  $t < -\eta$ ,  $\beta(t) = 1$  if  $t > \eta$ , and  $\beta^2(t) + \beta^2(-t) = 1$ . The window function can be constructed as

$$g_p^j(t) = \begin{cases} \beta(t - pM2^{-j}), & \text{if } t < pM2^{-j} + \eta, \\ 1, & \text{if } pM2^{-j} + \eta \leq t \leq (p+1)M2^{-j} - \eta, \\ \beta((p+1)M2^{-j} - t), & \text{if } t > (p+1)M2^{-j} - \eta, \end{cases} \quad (21)$$

where  $M2^{-j} \geq 2\eta$ . (See Fig. 5 in [11] for the illustration of a full admissible binary tree with corresponding window functions.) Note that

<sup>1</sup>The local cosine function  $\phi_{p,k}(t)$  defined in (8) can be represented as  $\phi_{x_p, \xi_{p,k}}(t) = g_{x_p}(t) \cos(\xi_{p,k} t + \theta_{p,k})$  with  $x_p = \frac{1}{2}(t_p + t_{p+1})$ ,  $g_{x_p}(t) = \sqrt{\frac{2}{l_p}} g_p(t)$ ,  $\xi_{p,k} = \frac{\pi(k+1/2)}{l_p}$  and  $\theta_{p,k} = -\xi_{p,k} t_p$ .

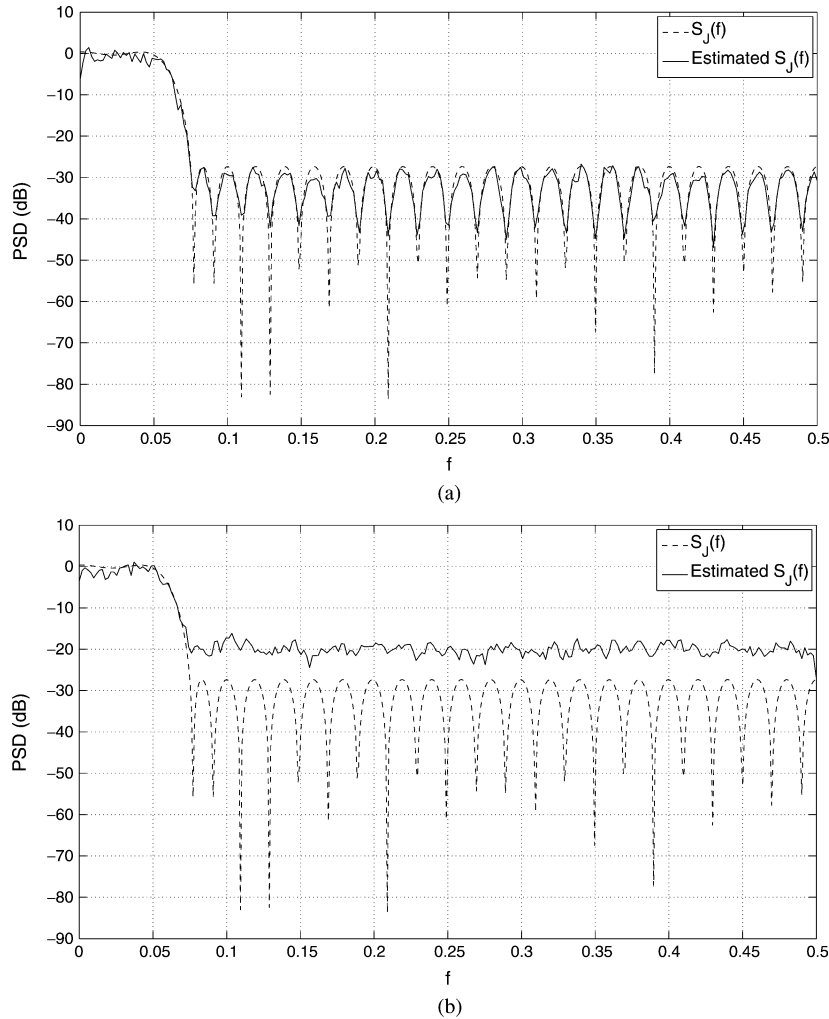


Fig. 2. Example 1: The true and estimated jamming power spectral density  $S_J(f)$ . (a) Noise-free case; (b) Noisy case; JNR = 10 dB.

the window function  $g_p^j(t)$  is associated with the local cosine family through

$$\left\{ \phi_{p,k}^j(t) = g_p^j(t) \sqrt{\frac{2}{M2^{-j}}} \cos \left[ \pi \left( k + \frac{1}{2} \right) \frac{t - M2^{-j}p}{M2^{-j}} \right] \right\} \quad (22)$$

where  $0 \leq k < M2^{-j}$ . For leaf nodes from the admissible binary tree indexed by  $\gamma$ , i.e.,  $(p, j) \in \gamma$ , the local cosine family  $\mathcal{B}^\gamma = \{\phi_{p,k}^j(t)\}_{(p,j) \in \gamma, 0 \leq k < M2^{-j}}$  formulates an orthogonal basis [12]. The dictionary  $\mathcal{D} = \{\mathcal{B}^\gamma\}_{\gamma \in \Gamma}$  is constructed with all admissible binary trees of depth no more than  $N_D$ .

2) *Best Basis Search Using Dynamic Programming:* Let  $C(p, j) = \sum_{k=0}^{M2^{-j}-1} |\hat{d}_{p,k}^j|^2$ . The Hilbert–Schmidt norm of the diagonal operator  $B_0^\gamma$  defined in (12) can be estimated as  $\|B_0^\gamma\|_h^2 = \sum_{(j,p) \in \gamma} C(p, j)$ . To obtain the best basis, we need to search in the dictionary for best basis that maximizes  $\|B_0^\gamma\|_h^2$ . Let  $\mathcal{B}_j^p$  denote the set of basis functions  $\{\phi_{p,k}^j(t)\}_{0 \leq k < M2^{-j}}$  and  $\mathcal{O}_j^p$  the set of best basis functions associated with node  $(p, j)$ . It can be shown that  $\|B_0^\gamma\|_h^2$  is maximized if we construct the  $\mathcal{O}_j^p$  using the following rule [12]:

$$\mathcal{O}_j^p = \begin{cases} \mathcal{O}_{j+1}^{2p} \cup \mathcal{O}_{j+1}^{2p+1}, & \text{if } C(p, j) < C(2p, j+1) \\ & + C(2p+1, j+1), \\ \mathcal{B}_j^p, & \text{otherwise.} \end{cases} \quad (23)$$

By making best basis selection at each node recursively using bottom-up progression, the overall best basis can be determined at the

root node  $\mathcal{B}^{\gamma_0} = \mathcal{O}_0^0$ . The computational complexity of the best basis search is reduced to  $O(M[\log_2 M]^2)$ . The best basis search scheme is summarized in Algorithm 1.

---

**Algorithm 1:** The Best Basis Search Algorithm

---

```

for  $j = (J - 1) : -1 : 0$  and  $p = 0 : (2^j - 1)$  do
    Compute  $C(p, j) = \sum_{k=0}^{M2^{-j}-1} |\hat{d}_{p,k}^j|^2$ 
    if  $j == J - 1$  then
        Mark node  $(p, j)$  as leaf
    else
        if  $C(p, j) \geq C(2p, j+1) + C(2p+1, j+1)$  then
            Mark node  $(p, j)$  as leaf
        else
            Leave node  $(p, j)$  unmarked and
             $C(p, j) = C(2p, j+1) + C(2p+1, j+1)$ 
        end if
    end if
end for
    
```

---

*Remark 1:* In literature, discussions on spectrum estimation for non-stationary signals have generally been limited to the cases where the signal can somehow be “mapped to” a stationary process. For example,

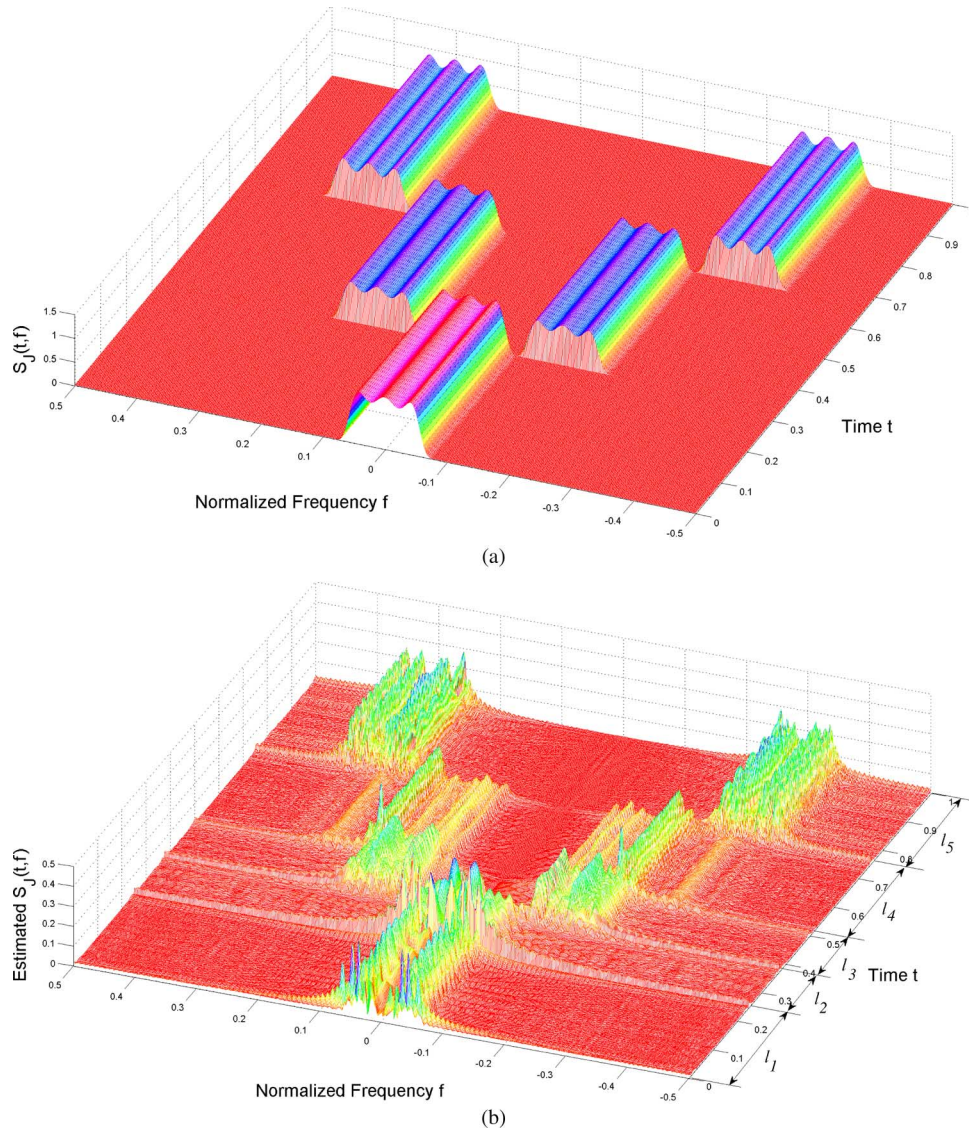


Fig. 3. Example 2: The true PSD and the PSD estimated under noisy environment. (a) True  $|S_J(t, f)|$  and (b) Estimated  $|S_J(t, f)|$ .

the “evolutionary spectral analysis” deals with a non-stationary spectrum whose physical interpretation is similar to that of a stationary spectrum. In this correspondence, we limit our discussion on non-stationary jamming to *locally stationary jamming*. Interested readers can find more information about this topic in [13] and [14].

#### IV. SIMULATION RESULTS

In this section, we illustrate the estimation of the time-varying jamming coherence time and the time-frequency jamming coherence bandwidth through simulation examples.  $M = 4096$  samples are obtained from the random jamming process, which is assumed to be real-valued zero-mean Gaussian. The time duration of the jamming is normalized to 1, and the frequency is normalized by the sampling rate. The jamming-to-noise ratio (JNR) is defined as the ratio of the jamming power to the noise power.

*Example 1—Stationary Jamming:* The jamming here has coherence time  $T_c = \frac{7}{4096}$ , and coherence bandwidth  $B_c(0) = 0.1056$ . We consider both the noise-free case and noisy case with JNR = 10 dB. We use the Welch–Bartlett method [15] to estimate the jamming PSD  $S_J(f)$ , and choose  $\alpha_0 = 0.5$ ,  $\alpha_1 = 0.95$ . The true and estimated  $S_J(f)$  are illustrated in Fig. 2. In the noisy case, the estimated jamming

coherence time and bandwidth are  $\hat{T}_c = \frac{6}{4096}$  and  $\hat{B}_c(0) = 0.1055$ , respectively.

*Example 2—Locally Stationary Jamming:* In this example, the jamming consists of 3 stationary intervals with equal length. The JNRs in the three intervals are set to be (10, 15, 15)dB, respectively, and the normalized center frequencies of  $S_J(t, f)$  in the three intervals are (0,0.15,0.3), respectively. The estimated best basis consists of local cosine functions associated with 5 different window supports, corresponding to intervals  $l_1 \sim l_5$ . The true and estimated  $|S_J(t, f)|$  are illustrated in Fig. 3, respectively. It can be observed that  $|\hat{S}_J(t, f)|$  concentrates within the same time-frequency areas as  $|S_J(t, f)|$ . Take  $t = 0.4375$  and  $v = 0.15$  as an example,  $T_c(0.4375) = \frac{2}{4096}$  and  $B_c(0.4375, 0.15) = 0.0801$ . With  $\alpha_0 = 0.5$ ,  $\alpha_1 = 0.7$ , the estimated results are:  $\hat{T}_c(0.4375) = \frac{1}{4096}$  and  $\hat{B}_c(0.4375, 0.15) = 0.0762$ .

#### V. CONCLUSION

This correspondence provides a 2D framework for cognitive jamming modeling and classification, through which all the existing jamming models can be summarized and extended to the time-varying case under one general scheme. By analyzing the time varying power spectral density, we introduce the concepts of time-varying jamming

coherence time and coherence bandwidth, and classify jamming as fast versus slow jamming, and flat versus frequency selective jamming. We provide specific methods on PSD estimation for time-varying jamming that is stationary or locally stationary. Classification for non-stationary jamming that is not locally stationary still needs further investigation.

## REFERENCES

- [1] R. Pickholtz, D. Schilling, and L. B. Milstein, "Theory of spread spectrum communications—A tutorial," *IEEE Trans. Commun.*, vol. 30, pp. 855–884, May 1982.
- [2] M. Pursley and W. Stark, "Performance of Reed–Solomon coded frequency-hop spread-spectrum communications in partial-band interference," *IEEE Trans. Commun.*, vol. 33, pp. 767–774, Aug. 1985.
- [3] B. Levitt, "FH/MFSK performance in multitone jamming," *IEEE J. Sel. Areas Commun.*, vol. 3, no. 5, pp. 627–643, 1985.
- [4] J.-W. Moon, J. Shea, and T. Wong, "Jamming estimation on block-fading channels," in *Proc. IEEE Military Commun. Conf.*, Oct. 31–Nov. 3, 2004, vol. 3, pp. 1310–1316.
- [5] N. Pronios and A. Polydoros, "Jamming optimization in fully-connected, spread-spectrum networks," in *Proc. IEEE Military Commun. Conf.*, pp. 65–70.
- [6] M. Pursley and J. Skinner, "Turbo product coding in frequency-hop wireless communications with partial-band interference," in *Proc. IEEE Military Commun. Conf.*, Oct. 2002, vol. 2, pp. 774–779.
- [7] L. Zhang, H. Wang, and T. Li, "Jamming resistance reinforcement of message-driven frequency hopping," in *Proc. Intl. Conf. Acoust., Speech, Signal Process.*, Mar. 2010, pp. 3974–3977.
- [8] M. Priestley, "Evolutionary spectra and non-stationary processes," *J. Roy. Stat. Soc.*, ser. B, pp. 204–237, 1965.
- [9] R. Dahlhaus, "On the Kullback–Leibler information divergence of locally stationary processes," *Stoch. Process. Appl.*, vol. 62, no. 1, pp. 139–168, 1996.
- [10] T. Rappaport, *Wireless Communications—Principles and Practice*. Englewood Cliffs, NJ: Prentice-Hall, 2002.
- [11] S. Mallat, G. Papanicolaou, and Z. Zhang, "Adaptive covariance estimation of locally stationary processes," *Ann. Stat.*, vol. 26, no. 1, pp. 1–47, 1998.
- [12] R. Coifman and M. Wickerhauser, "Entropy-based algorithms for best basis selection," *IEEE Trans. Inf. Theory*, vol. 38, no. 2, pp. 713–718, Mar. 1992.
- [13] P. Flandrin, A. Napolitano, H. Ozaktas, and D. Thomson, Eds., "Recent advances in theory and methods for nonstationary signal analysis," *EURASIP J. Adv. Signal Process. (Special Issue)*, 2011, doi:10.1155/2011/963642.
- [14] W. Fitzgerald, R. Smith, A. Walden, and P. Young, Eds., *Nonlinear and Nonstationary Signal Processing*. Cambridge, U.K.: Cambridge Univ. Press, 2002.
- [15] D. Manolakis, V. Ingle, and S. Kogon, *Statistical and adaptive signal processing*. Norwood, MA: Artech House, 2005, vol. 1.

## Cooperative Localization and Tracking of Mobile Ad Hoc Networks

Liang Dong

**Abstract**—Cooperative localization and tracking technique relies on pairwise measurements to jointly estimate the positions and the velocities of multiple nodes in a mobile ad hoc network. The pairwise measurements include the range and the radial velocity between the transmitting and receiving nodes. For a large-scale network, we formulate the state-space models for the subsystems and develop the distributed extended Kalman filters for cooperative localization and tracking. The decentralized approach takes into account the limited resources of node memory, embedded computation, and communication bandwidth. The algorithm works well in a sparsely connected mobile network and can adapt to changes in network connectivity. Numerical results show that the performances of the decentralized cooperative localization and node velocity estimation are close to the posterior Cramér–Rao lower bounds of the centralized approach.

**Index Terms**—Adaptive signal processing, cooperative systems, distributed algorithms, estimation theory, Kalman filters, mobile ad hoc networks.

## I. INTRODUCTION

Without fixed infrastructure or centralized administration in a wireless ad hoc network, the knowledge of node positions plays an important role in network operation. Moreover, mobility awareness and management are essential in a mobile ad hoc network (MANET). Cooperative localization provides relative positions of wireless nodes based on pairwise measurements between the transmitting and receiving nodes [1], [2]. Multidimensional scaling (MDS) [3] can be used as an effective technique that transforms pairwise distance information into relative coordinates of nodes [4], [5]. Given the underlying statistical models of the range measurements, a maximum-likelihood estimator (MLE) can be used, trading complexity with accuracy [6], [7]. The maximum-likelihood estimator requires centralized data processing and there is no guarantee of global convergence. Multidimensional scaling can initialize the maximum-likelihood estimator to achieve superior performance [8]. Semidefinite programming relaxation to maximum-likelihood estimator formulation can be used to ensure a global solution. The localization problem can be formulated as a special case of the general semidefinite programming-based approach for solving the graph realization problem [9]. Doherty *et al.* introduced an approach to sensor position estimation that uses convex optimization [10]. Chan *et al.* derived subspace methods for node localization in a fully connected wireless network based on range measurements [11]. With a *prior* probability distribution of the node positions, Xi *et al.* employed a Bayesian minimum mean-square error (MMSE) estimator for cooperative localization [12]. Huang and Záruba designed a probabilistic localization method based on particle filtering for an ad hoc heterogeneous network where different nodes may have different sensory capacities [13].

In MANET, radial velocity between the transmitting and receiving nodes is an additional metric that can be exploited for cooperative lo-

---

Manuscript received May 23, 2011; revised September 21, 2011, November 30, 2011, and February 20, 2012; accepted March 07, 2012. Date of publication March 23, 2012; date of current version June 12, 2012. The associate editor coordinating the review of this manuscript and approving it for publication was Prof. Min Dong.

The author is with the Department of Electrical and Computer Engineering, Baylor University, Waco, TX 76798 USA (e-mail: liang\_dong@baylor.edu).

Color versions of one or more of the figures in this paper are available online at <http://ieeexplore.ieee.org>.

Digital Object Identifier 10.1109/TSP.2012.2191778